

# Momentum Transfer in Heavy-Ion-Induced Fission\*

TORBJØRN SIKKELAND, ELTON L. HAINES, AND VICTOR E. VIOLA, JR.  
Lawrence Radiation Laboratory, University of California, Berkeley, California

(Received September 7, 1961)

The forward linear momentum transfer in reactions leading to fission between heavy ions such as  $C^{12}$ ,  $N^{14}$ ,  $O^{16}$ , and  $Ne^{20}$  and the target nuclei  $Ho$ ,  $Au$ ,  $Bi$ , and  $U^{238}$  has been investigated by measuring the angular correlation between the fragments. The experimental values for the most probable parameters for center-of-mass transformation for these systems are compared with calculated values. For all the systems, the dominant reaction involves a full momentum transfer by the heavy ion to the fissioning nucleus. It is observed that for the system  $Au+Ne^{20}$  and  $Bi+Ne^{20}$ , reactions with incomplete momentum deposition contribute 5.1% and 8.6%, respectively, to the total fission cross section. For  $U^{238}$  targets this admixture amounts to 12 to 17% for all ions at the highest bombarding energy and decreases with decreasing projectile energy. Possible reaction mechanisms leading to fission are suggested. A brief discussion of the method and its application is given.

## INTRODUCTION

IN any model for a nuclear reaction, linear momentum must be conserved. It is therefore of importance to be able to perform a momentum analysis experimentally.

In the study of reactions that lead to fission, angular-distribution measurements of the fragments furnish average values for the forward momentum transferred by the ion to the fissioning nucleus. The distribution in the laboratory system is transformed to the coordinate system of the fissioning nucleus (from now on called the c.m. system) by use of the parameter  $x^2$ , defined as

$$x^2 = (v_{fN}/v_{ff})^2. \quad (1)$$

Here  $v_{fN}$  is the velocity component of the fissioning

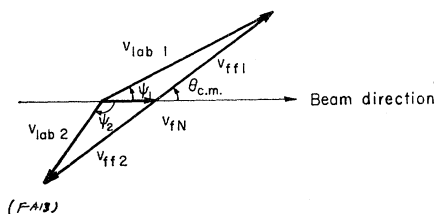


FIG. 1. Vector diagram of the relationship between the laboratory and center-of-mass systems in a binary fission event, where  $\psi$ ,  $\theta_{c.m.}$ ,  $v_{ff}$ , and  $v_{fN}$  are defined in the text. The laboratory velocities of the fission fragments are defined by  $v_{lab 1}$  and  $v_{lab 2}$ .

nucleus along the beam axis, and  $v_{ff}$  is the velocity of the fission fragment in the c.m. system (see Fig. 1). This transformation yields mean values of  $x^2$ ,  $x_m^2$ .<sup>1-3</sup> The same value is obtained by measuring the median range of fission fragments in emulsion vs laboratory angle.<sup>4</sup> Alexander and Gadzik measured ranges of

fragments in aluminum in the forward and backward directions, from which average values for  $v_{fN}$  could be deduced.<sup>5</sup>

By measuring the most probable fragment kinetic energy in the laboratory system  $E_L$ , as a function of angle one can evaluate  $x_m^2$ , the most probable value for  $x^2$ .<sup>2</sup> The values obtained with these methods are not very accurate, however. They are insensitive for the detection of components in a mixture of reactions involving varying degrees of momentum transfer.

Indications for reactions with incomplete momentum deposition, from now on called non-compound-nucleus (NCN) reactions, have been observed for the system  $U^{238}+C^{12}$ .<sup>2</sup> For that system, any reaction depositing more than 5-Mev excitation energy leads in most cases, to fission. For lighter elements, the fission thresholds are higher and fission occurs only for compound-nucleus (CN) reactions in which the heavy ion amalgamates with the target nucleus, or other reactions in which large excitations are produced. The investigation reported here was undertaken with a technique expected to be more sensitive and more direct in the analysis of the  $x^2$  values.<sup>6</sup>

The method consists of measuring the fragment-fragment coincidence rate as a function of the angular positions  $\psi_1$  and  $\psi_2$  of the fragments relative to the beam axis. With the detectors placed on opposite sides and in the plane of the beam axis, the conditions for coincidence are (see Fig. 1)

$$\tan\psi_1 = \sin\theta_{c.m.}/(x_1 + \cos\theta_{c.m.}), \quad (2)$$

$$\tan\psi_2 = \sin\theta_{c.m.}/(x_2 - \cos\theta_{c.m.}). \quad (3)$$

Here  $x$  is as defined before and  $\theta_{c.m.}$  is the c.m. angle. For one value of  $v_{fN}$  conditions (2) and (3) are fulfilled for a variety of  $(x_1, x_2)$  values because of the wide spread in the velocity of the fragments, giving coincidences over a range of  $\psi_1$  and  $\psi_2$ . For high-energy fission, symmetric division is the most probable mode.

\* This work was done under the auspices of the U. S. Atomic Energy Commission.

<sup>1</sup> G. E. Gordon, A. E. Larsh, T. Sikkeland, and G. T. Seaborg, Phys. Rev. **120**, 1341 (1960).

<sup>2</sup> T. Sikkeland, A. E. Larsh, and G. E. Gordon, Phys. Rev. **123**, 2112 (1961).

<sup>3</sup> Victor E. Viola, Jr., thesis, University of California Radiation Laboratory Report UCRL-9619, 1961 (unpublished).

<sup>4</sup> E. Goldberg, H. L. Reynolds, and D. D. Kerlee, in *Proceedings of the Second Conference on Reactions between Complex Nuclei*, Gatlinburg, Tennessee (John Wiley & Sons, Inc., New York, 1960) p. 230.

<sup>5</sup> J. M. Alexander and M. F. Gadzik, in Chemistry Division Annual Report for 1960, University of California Radiation Laboratory Report UCRL-9566, 1961 (unpublished), p. 145.

<sup>6</sup> W. J. Nicholson and I. Halpern, Phys. Rev. **116**, 175 (1959).

Because of conservation of momentum the fragment velocities are equal, therefore a maximum coincidence rate is expected for  $x_1 = x_2 = x_{mp}$ . The most probable  $x^2$  value,  $x_{mp}^2$ , can thus be determined. If several  $v_{fN}$  values are present, the curve is expected to exhibit more than one peak.

### EXPERIMENTAL PROCEDURE

Heavy-ion beams were obtained from the Berkeley heavy-ion linear accelerator (Hilac), which accelerates ions to  $10.4 \pm 0.2$  Mev/nucleon.<sup>7</sup> The beam was deflected through 15 deg by a bending magnet before reaching the fission and scatter chamber, which is shown in Fig. 2. Lower energies were obtained by inserting weighed aluminum foils into the beam path. Measured range-energy curves for aluminum were used to estimate the resulting energy.<sup>8</sup>

Before striking the target, the beam passed through two  $1.5 \times 6$ -mm collimators 25 in. apart. The last collimator was  $2\frac{1}{4}$  in. from the target. Beam particles were collected in a 3-in.-wide Faraday cup at the rear of the chamber. In front of the cup was a permanent magnet which prevented electrons from entering or leaving the cup.

Targets were either self-supporting or supported by  $100\text{-}\mu\text{g}/\text{cm}^2$  thick nickel films. Target thicknesses were generally around  $200\text{-}\mu\text{g}/\text{cm}^2$ . The target was mounted in the center of the tank and its orientation with respect to the beam could be changed.

The detectors used were silicon diode crystals covered with Au, about  $50\text{ }\mu\text{g}/\text{cm}^2$  thick.<sup>9</sup> They were mounted on arms which could be moved independently of each other around the center of the tank in all directions except for approximately 10 degrees in the backward direction. The distances of the detectors from the target, and their angular positions could be adjusted while the

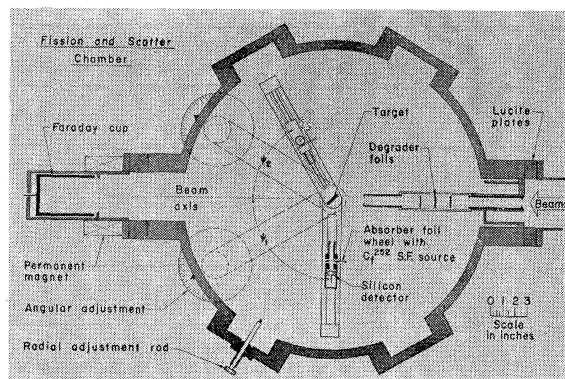


FIG. 2. Schematic diagram of the fission and scatter chamber.

tank was under vacuum. In front of the detectors was a collimating system which defined the geometry. The angular position of each detector was determined to  $\pm \frac{1}{4}$  deg by counting elastically scattered heavy ions on each side of the beam axis.

The electronic system (Fig. 3) consisted of two linear amplifier systems and a fast-coincidence system. The "slow" pulse (1  $\mu\text{sec}$  width) from each crystal was passed through a preamplifier in the bombardment area and then to a doubly differentiating linear amplifier in the counting area. The amplified signals were transmitted to variable-delay and gate units and then into individual scalars and a transistorized coincidence unit. The "fast" pulse (4-nsec width) from each crystal was passed through two distributed amplifiers in the bombardment area and then to the counting area by way of high-impedance cables. After further amplification, the pulses were fed through a transistorized fast-coincidence unit. The output pulse from this unit was led through a 10-megacycle discriminator-scaler and a

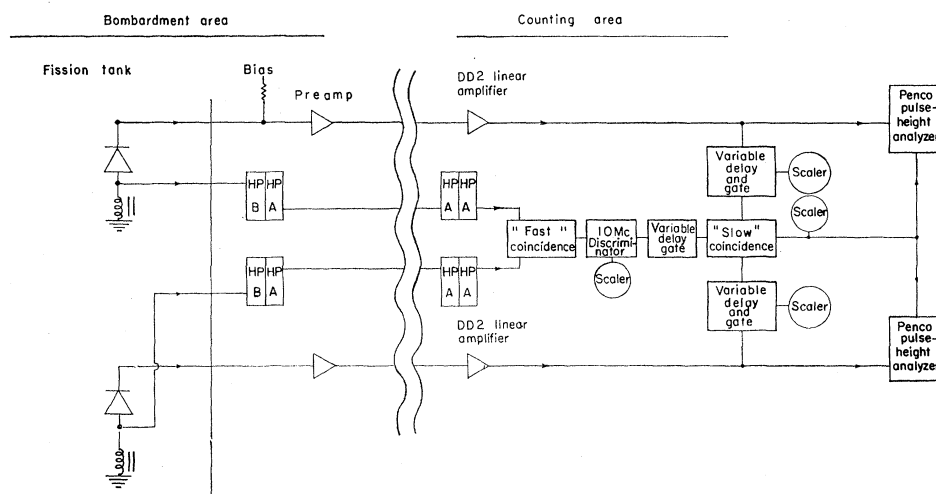


FIG. 3. Electronic system used in the angular correlation experiments.

<sup>7</sup> E. L. Hubbard, W. R. Baker, K. W. Ehlers, *et al.*, University of California Radiation Laboratory Report, UCRL-9453, 1960 (unpublished).

<sup>8</sup> L. C. Northcliffe, *Phys. Rev.* **120**, 1744 (1960).

<sup>9</sup> Robert M. Latimer, Lawrence Radiation Laboratory, 1961 (unpublished work).

TABLE I. Measured and calculated properties of each fissioning system studied in this work.  $W_{\frac{1}{2}}$  is the angular width at half maximum for the angular correlation.<sup>a</sup> Other symbols are defined in the text.

Heavy ion	Target	Heavy-ion energy (Mev)	$\psi_1$ (deg)	$\psi_{2mp}$ (deg)	$W_{\frac{1}{2}}$ (deg)	$x_{mp}^2$	NCN (%)	$E_{c.m.}$ (Mev)	$A_{ff}$ (amu)	$\bar{x}_{CN}^2$
C <sup>12</sup>	Ho <sup>165</sup>	125	90	61.6	6.5	0.068	0	63 <sup>b</sup>	82.2	0.062
	Au <sup>197</sup>	125	90	66.8	7.3	0.044	0	73 <sup>c</sup>	98.5	0.046
	Bi <sup>209</sup>	125	90	68.0	6.6	0.039	0	78 <sup>b</sup>	105.3	0.041
	U <sup>238</sup>	125	90	70.2	7.0	0.031	11.9%	91 <sup>d</sup>	117.6	0.031
	U <sup>238</sup>	93.7	90	72.4	6.8	0.025	1.8%	91 <sup>d</sup>	119.3	0.024
	U <sup>238</sup>	74.8	90	74.3	6.2	0.019	0	91 <sup>d</sup>	120.4	0.019
N <sup>14</sup>	Au <sup>197</sup>	145	90	64.4	7.9	0.054	~0	74 <sup>b</sup>	98.4	0.061
	Bi <sup>209</sup>	145	90	65.9	7.7	0.052	~0	79 <sup>b</sup>	105.2	0.055
	U <sup>238</sup>	145	90	68.2	7.1	0.039	16.9%	92 <sup>b</sup>	117.4	0.041
	U <sup>238</sup>	145	40	122.5	8.0	0.042	8.7%	92 <sup>b</sup>	117.4	0.041
	U <sup>238</sup>	103	90	71.2	6.7	0.028	4.8%	92 <sup>b</sup>	119.1	0.028
	Ho <sup>165</sup>	166	90	54.7	7.8	0.111	0	65 <sup>c</sup>	81.8	0.102
O <sup>16</sup>	Au <sup>197</sup>	166	90	60.5	7.8	0.074	~1%	75 <sup>c</sup>	99.0	0.077
	Bi <sup>209</sup>	166	90	62.1	6.2	0.066	~0	80 <sup>c</sup>	104.8	0.069
	U <sup>238</sup>	166	90	64.6	7.1	0.053	15.7%	93 <sup>c</sup>	117.8	0.052
	U <sup>238</sup>	166	40	120.4	8.6	0.052	8.4%	93 <sup>c</sup>	117.8	0.052
	U <sup>238</sup>	140	90	66.6	7.6	0.045	10.2%	93 <sup>c</sup>	119.3	0.045
	U <sup>238</sup>	110	90	68.8	6.2	0.036	3.2%	93 <sup>c</sup>	121.0	0.035
Ne <sup>20</sup>	Au <sup>197</sup>	207	90	55.3	9.5	0.107	5.1%	77 <sup>b</sup>	99.8	0.111
	Bi <sup>209</sup>	207	90	57.0	9.0	0.095	8.6%	82 <sup>b</sup>	106.1	0.095
	U <sup>238</sup>	207	90	60.8	7.9	0.072	16.4%	95 <sup>b</sup>	118.3	0.078

<sup>a</sup> Uncorrected for angular resolution.  
<sup>c</sup> This work.

<sup>b</sup> Estimated.  
<sup>d</sup> Reference 2.

<sup>e</sup> Reference 11.

variable-delay and gate unit into the coincidence unit used by the linear system. Thus three-way coincidence was demanded between two linear pulses and a fast coincidence pulse. The output pulse of this coincidence unit drove a scaler and was used as a gate pulse for two Penco 100-channel pulse-height analyzers to analyze the linear pulses. The use of fast coincidence reduced the accidentals to a negligible rate, even with one

detector at a forward angle where large numbers of beam particles were detected.

### ENERGY MEASUREMENTS

In order to interpret the results, determination of the most probable kinetic energy of the fragments was necessary. Previous results have shown a defect in the energy spectrum of the fragments from the spontaneous fission of Cf<sup>252</sup> as observed with a silicon detector.<sup>2</sup> An attempt was therefore made to obtain a more reliable curve of energy vs pulse height for such a detector. For that purpose, the most probable laboratory-system kinetic energy,  $E_L$ , of the fragments from fission induced by heavy ions was used as a convenient calibration source.  $E_L$  varies with angle according to the equation

$$E_L = E_{c.m.}(1 + x_{mp}^2 + 2x_{mp} \cos \theta_{c.m.}). \quad (4)$$

The  $\theta_{c.m.}$ , the c.m. angle, is related to the lab angle  $\psi$  by Eq. (2);  $E_{c.m.}$  is the most probable kinetic energy in the c.m. system after the prompt neutron emission, and is to a good approximation a constant independent of  $\theta_{c.m.}$ . Values for  $x_{mp}^2$ , the most probable  $x^2$  value, for several systems are measured directly and to a high accuracy in this investigation, as is shown in the next section. We decided to use the system Au+166-Mev O<sup>16</sup> for calibration, since this gives a wide range of  $E_L$ . The  $x_{mp}^2$  value as given in Table I is  $0.074 \pm 0.002$ .

The variation of  $E_L$  with  $\psi$  is known by determining the angle at which the pulse height is equal to the most probable pulse height produced by the light fragments from a Cf<sup>252</sup> source. At that position  $E_L = 103$  Mev, which is the most probable kinetic energy (corrected

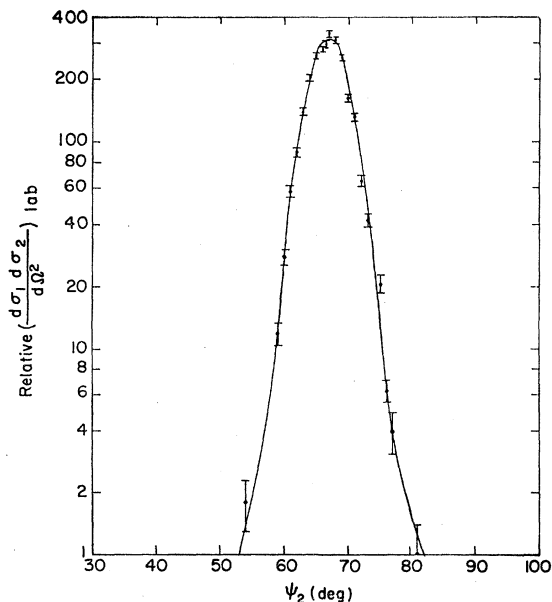


FIG. 4. Fission-fragment angular correlation for the system 125-Mev C<sup>12</sup>+Au<sup>197</sup>.  $\psi_1$  at 90 deg.

for energy loss due to evaporated neutrons) of the light-fragment group as determined with the time-of-flight technique.<sup>10</sup> This peak was chosen because the values for the most probable mass,  $A_{ff}$ , from the two sources are comparable (110 for  $\text{Cf}^{252}$  and 100 for  $\text{Au} + 166\text{-Mev O}^{16}$ ). In both cases the fragments suffer the same energy degradation in the Au "window" of the crystal. The energy degradation in the  $200\text{-}\mu\text{g}/\text{cm}^2$  Au target was determined experimentally by placing the target surface first parallel and then at  $45^\circ$  to the surface of the crystal. The correction to "zero thickness" was found to be about 1 Mev.

The heavy-fragment group from  $\text{Cf}^{252}$  has a most probable mass of 140 and a kinetic energy of 79 Mev. It is interesting to note that a fragment with mass 100 and the same energy gives a higher pulse height. At this energy, there appears to be a "mass effect" of approximately 70 keV/nucleon. From Table I it is seen that the fragments we are dealing with have  $A_{ff}$  ranging from 100 to 120 amu, and the mass-defect correction should therefore be comparable. The quantity in which we are interested is  $E_{o.m.}$ . Because  $x_{mp}^2$  is determined experimentally by another method,  $E_{o.m.}$  is found by measuring  $E_L$  for one position of the detector. To avoid the possibility that the "mass defect" might vary with energy, a position was chosen which yielded an  $E_L$  close to 79 Mev. The over-all error in the value for  $E_{o.m.}$  obtained by this method is believed to be less than 4%.

### RESULTS AND DISCUSSION

In the coincidence measurements, one of the detectors was placed at a fixed position  $\psi_1$ , while the angle of the

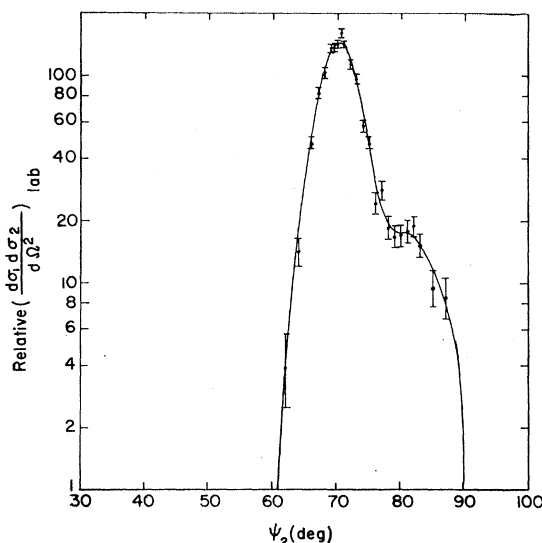


FIG. 5. Fission-fragment angular correlation for the system 125-Mev  $\text{C}^{12} + \text{U}^{238}$ ,  $\psi_1$  at  $90^\circ$ .

<sup>10</sup> J. S. Fraser and J. C. D. Milton, in *Proceedings of the Second United Nations International Conference on the Peaceful Uses of Atomic Energy, Geneva, 1958* (United Nations, New York, 1958), Vol. 15, p. 216.

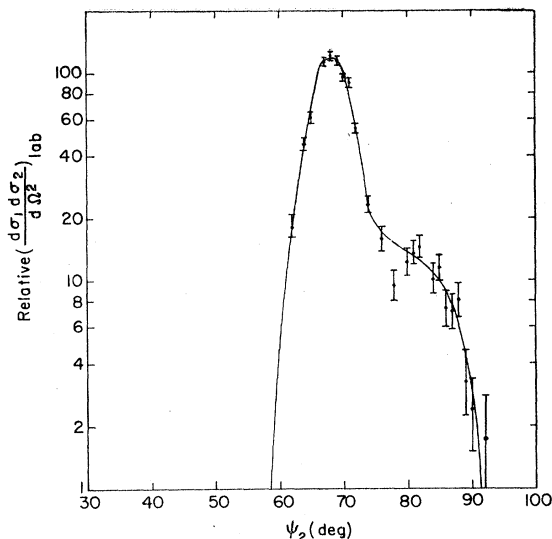


FIG. 6. Fission-fragment angular correlation for the system 145-Mev  $\text{N}^{14} + \text{U}^{238}$ ,  $\psi_1$  at  $90^\circ$ .

other detector  $\psi_2$  was varied. In most of the experiments  $\psi_1$  was set at  $90^\circ$ . In a few cases  $\psi_1 = 40^\circ$  was also chosen in order to investigate any angular variation. The finite width of the collimator accounted for an angular spread of  $\pm 0.5^\circ$  and that of the detector geometry for  $\pm 1.0^\circ$ .

Curves for some of the systems investigated are reproduced in Figs. 4 through 13. Generally the curves can be divided into two groups. In the first group the curves are characterized by a symmetric peak with a half-width around 6 to 9 deg. Corrected for angular resolution, this corresponds to an intrinsic half-width

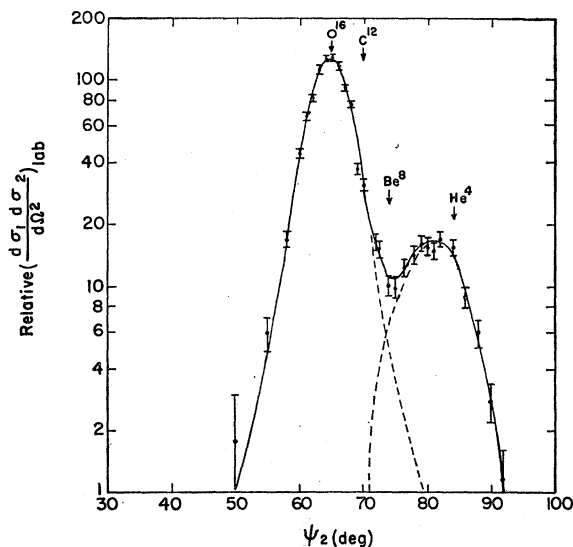


FIG. 7. Fission-fragment angular correlation for the system 166-Mev  $\text{O}^{16} + \text{U}^{238}$ ,  $\psi_1$  at  $90^\circ$ . Each arrow represents the estimated peak position for the capture of the indicated fragment from the incident heavy ion.

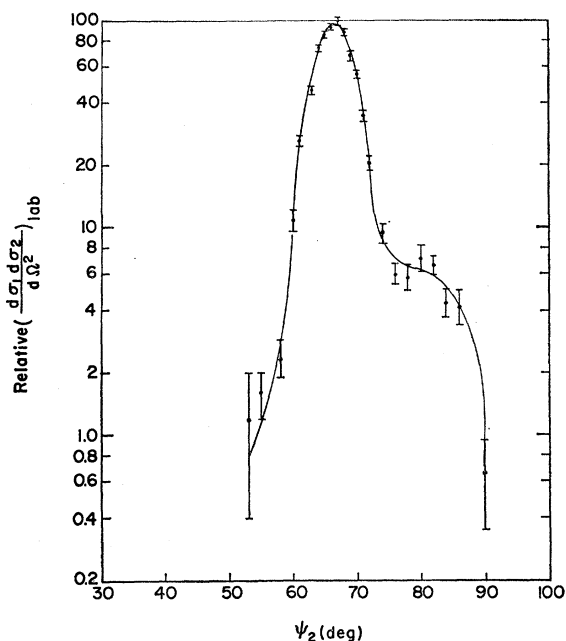


FIG. 8. Fission-fragment angular correlation for the system 140-Mev  $O^{16} + U^{238}$ ,  $\psi_1$  at 90 deg.

of 4.5 to 8 deg. To this group belong the Ho, Au, and Bi targets and also the system  $U^{238} + 75$ -Mev  $C^{12}$  ions. Figure 4 shows the system  $Au + C^{12}$  which is typical for this group. In regard to the total coincidence curve, the appearance of a symmetric peak is expected in a

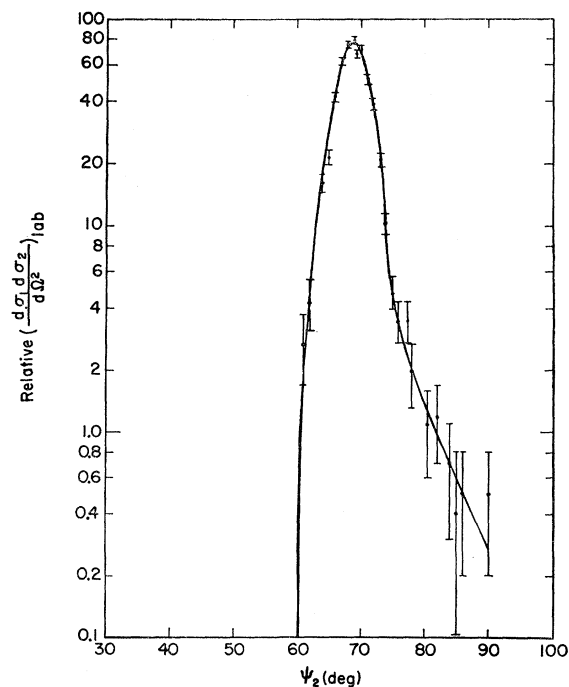


FIG. 9. Fission-fragment angular correlation for the system 110-Mev  $O^{16} + U^{238}$ ,  $\psi_1$  at 90 deg.

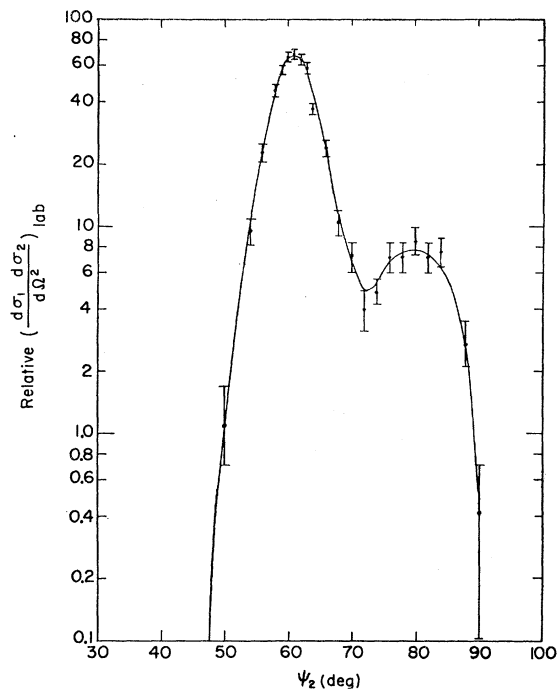


FIG. 10. Fission-fragment angular correlation for the system 207-Mev  $Ne^{20} + U^{238}$ ,  $\psi_1$  at 90 deg.

case with specific momentum transfer followed by symmetric fission. Coincidence curves of the other group are characterized by an asymmetric peak. Some typical curves are shown in Figs. 5 through 13. In this group, we see that for the same bombarding energy, the peak becomes more distorted as the masses of the target and projectile increase. The distortion is toward higher angles, which correspond to lower  $x^2$  values.

We first consider the main peak. At the peak, as we have discussed before,  $x_1 = x_2 = x_{mp}$ . Values for  $x_{mp}^2$  for Groups I and II are given in Table I. The uncertainty of the values is of the order of  $\pm 3\%$ , corresponding to a  $\pm \frac{1}{4}$ -deg uncertainty in the position of the peak. As is seen from Table I,  $x_{mp}^2$  does not seem to vary with angle.

In the following we compare the experimentally determined  $x_{mp}^2$  with estimated most probable values,  $\bar{x}_{CN}^2$ . For such a reaction, assuming the particles emitted before fission are evaporated,  $\bar{x}_{CN}^2$  for a CN is given by

$$\bar{x}_{CN}^2 = A_I E_I A_{ff} / A_{CN}^2 E_{e.m.}, \quad (5)$$

where  $A_I$  is the mass and  $E_I$  the lab kinetic energy of the heavy ion;  $A_{CN}$  is the mass of the compound nucleus;  $A_{ff}$  and  $E_{e.m.}$  are as defined before. Because the prompt neutrons emitted in the fission process presumably are isotropic in the framework of the fragments, final values for  $A_{ff}$  and  $E_{e.m.}$  can be used. Values for  $E_{e.m.}$  after prompt neutron emission, for some of the systems studied here, have been measured by several groups.<sup>1,2,11</sup> In cases in which no data were available, energy measurements were carried out as shown under "Energy

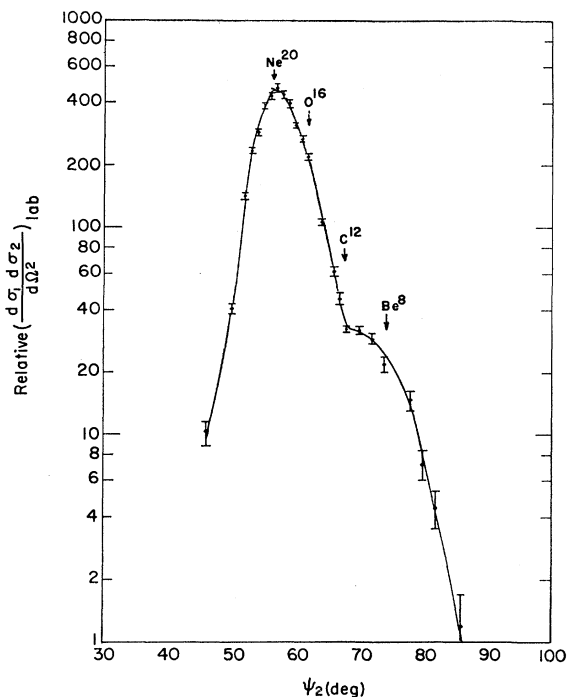


FIG. 11. Fission-fragment angular correlation for the system 207-Mev  $\text{Ne}^{20} + \text{Bi}^{209}$ ,  $\psi_1$  at 90 deg. Each arrow represents the estimated peak position for the capture of the indicated fragment from the incident heavy ion.

Measurements".  $E_{o.m.}$  is known to within 4%.  $A_{ff}$  was estimated by assuming a symmetric division. We then have  $A_{ff} = \frac{1}{2}(A_{fN} - \bar{\nu})$  where  $A_{fN}$  is the mass of the fissioning nucleus and  $\bar{\nu}$  the mean number of neutrons

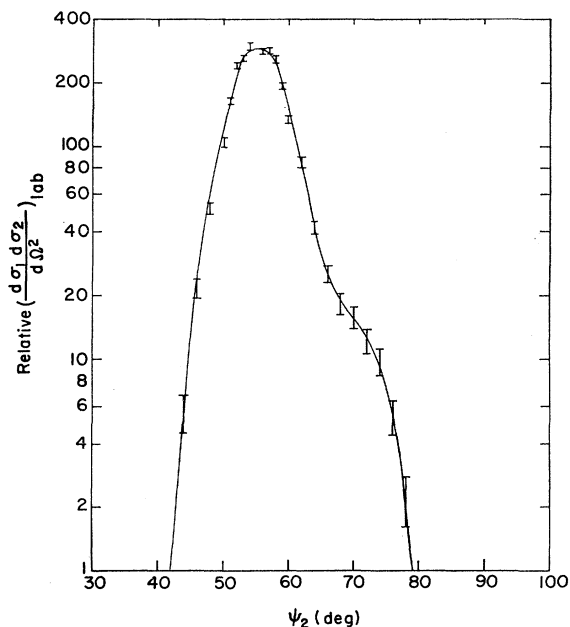


FIG. 12. Fission-fragment angular correlation for the system 207-Mev  $\text{Ne}^{20} + \text{Au}^{197}$ ,  $\psi_1$  at 90 deg.

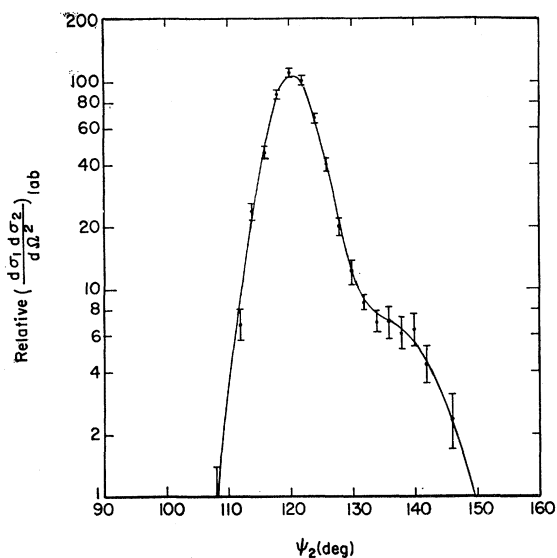


FIG. 13. Fission-fragment angular correlation for the system 166-Mev  $\text{O}^{16} + \text{U}^{238}$ ,  $\psi_1$  at 40 deg.

emitted in the fission process;  $\bar{\nu}$  is estimated from Leachman's relationship,<sup>12</sup>

$$\bar{\nu} = \bar{\nu}_0 + 0.12E, \quad (6)$$

where  $E$  is the excitation energy of the fissioning nucleus in Mev and  $\bar{\nu}_0$  the mean number of neutrons emitted in spontaneous fission. The  $\bar{\nu}_0$  varies with  $Z$  and  $A$  in a systematic manner. Values for  $\bar{\nu}_0$  were taken from the compilations by Huizenga and Vandenbosch.<sup>13</sup> Early in the evaporation chain, the fissioning nucleus has a higher mass but also a higher excitation energy, which results in emission of a larger number of neutrons in the fission process than later in the chain.  $A_{ff}$  therefore shows a small variation along the chain. The calculated values given in Table I are averages for the whole chain. Experimental values exist only for the system  $\text{Au} + 114\text{-Mev C}^{12}$ . Blann gives the value  $97.5 \pm 2.5$  for  $A_{ff}$ ,<sup>14</sup> which is to be compared to the estimated value of 98.5. This, then, gives an idea of the errors involved. The over-all uncertainty in the calculated values for  $x_{\text{CN}}^2$  given in Table I is of the order of 5%. The agreement between  $x_{m_p}^2$  and  $\bar{x}_{\text{CN}}^2$  is therefore to be regarded as satisfactory. The CN reaction thus is the most probable event for both groups.

It is reasonable to assume that the CN reactions in Group II should give symmetric coincidence curves similar to those in Group I. We further assume that towards lower angles of the peak (at higher  $x^2$  values),

<sup>11</sup> H. C. Britt and A. R. Quinton, *Phys. Rev.* **120**, 1768 (1960).

<sup>12</sup> R. B. Leachman, in *Proceedings of the Second International Conference on the Peaceful Uses of Atomic Energy, Geneva, 1958* (United Nations, New York, 1958), Vol. 15, p. 229.

<sup>13</sup> J. R. Huizenga and R. Vandenbosch, in *Nuclear Reactions* [North-Holland Publishing Company, Amsterdam (to be published)], Vol. 2.

<sup>14</sup> H. Marshall Blann, thesis, University of California Radiation Laboratory Report, UCRL-9190, (unpublished).

the events are coming from CN reactions. We have accordingly constructed complete CN curves. These curves also have half-widths of about 6 to 8 deg. A curve representing NCN reactions is then obtained by subtracting the total CN curve from the total coincidence curve. This is shown for the  $O^{16}+U^{238}$  system in Fig. 7. The percent contributions from NCN reactions to the total fission cross section were obtained by integrating the area of both the CN and the NCN contributions and are given in Table I. It appears that in all cases most of the events proceed as CN reactions. The ratio for the NCN reaction is lower at 40 deg than at 90 deg, indicating a more nearly isotropic distribution of the fragments from this reaction. This is to be expected because the angular momentum deposited is less than for a CN reaction.<sup>2</sup>

Comparison with other results reveals that the number for % NCN reactions in Table I may be systematically too low. From spallation studies, it is estimated that the NCN reactions leading to fission contribute 20 to 30% to the reaction cross section.<sup>15-17</sup> This fraction does not vary appreciably with bombarding energy.

The reaction corresponding to the transfer of an alpha particle to the target nucleus dominated. Britt and Quinton have directly observed alpha particles and protons in reactions between heavy ions and targets such as Au and Bi.<sup>18</sup> They found the charged particles from NCN reactions to dominate over those from the CN reactions. The yield of the alphas was about three times that of the protons. At 10.5-Mev/nucleon bombarding energy, the cross section for emission of direct-interaction alpha particles was 25 to 35% of the total reaction cross section. For  $C^{12}$  the fraction decreased to 15% at the lowest bombarding energy of 85 Mev. Such reactions should lead to fission for a  $U^{238}$  target, because of its low fission barrier.

The discrepancy between these measurements probably lies in the insensitivity of the angular correlation method to separate reactions that have small differences in momentum transfer. To demonstrate this, we will attempt in the following to estimate  $x^2$  values for different NCN reactions. In order to do this, velocities and directions of the emitted particles must be known.

Britt and Quinton found the velocities of the direct-interaction alphas and protons to be close to the velocity of the incoming ion.<sup>18</sup> The particles were strongly peaked in the forward direction at maximum bombarding energy. For 85-Mev  $C^{12}$ , the peak decreases markedly.

We will now consider two extreme cases for the path of emitted particles having the same velocity as the heavy ion. In the first case, we let the particles proceed

parallel to the beam axis. We have indicated peak positions for possible reactions in Figs. 7 ( $O^{16}+U^{238}$ ) and 11 ( $Ne^{20}+Bi^{209}$ ) calculated for this case. In the second case, we assume that the emitted particles follow the path of the incoming heavy ion defined by the Coulomb orbit of the highest impact parameter. Accordingly, the momentum along the beam axis carried away by the emitted particle will decrease with decreasing bombarding energy. The  $x^2$  values for the NCN reactions will approach those of the CN reaction and at the Coulomb barrier will be even higher.

We can now compare the estimated values for the two cases with the experimental value for the reaction between  $U^{238}$  and 166-Mev  $O^{16}$ . The observed peak position for the NCN peak corresponds to a transfer of 30% of the forward momentum of the heavy ion. This peak should be coming predominantly from an alpha-transfer reaction. We calculate then that 25% of the projectile momentum will be transferred to the target nucleus if the stripped ion is emitted along the beam axis, and 35% if it is emitted along the Coulomb orbit. Apparently the average event is between the two extreme cases, and the emitted particles exchange some of their momenta with the struck nucleus. This may explain in particular the discrepancy for the lowest bombarding energies of  $U^{238}$ , where this exchange should be quite large. The numbers for % NCN given in Table I therefore must be regarded as lower limits. A separation of different reactions is only feasible at the highest bombarding energies where large differences in  $x^2$  occur.

It appears that reactions involving the transfer of one  $\alpha$  particle to the target nucleus are not observed for the reactions with  $Ne^{20}$  incident on Au and Bi targets. Such reactions do not deposit high enough excitation energy in the residual nucleus for it to undergo fission, because the fission threshold is so high that the level width for fission is too low to allow fission to be detected. However, the transfer of larger fragments can contribute a substantial amount of fission, as is indicated in the curves.

We now discuss the NCN curve for  $U^{238}$  and 166-Mev  $O^{16}$  in more detail. We notice that the half-width of the peak is larger than that observed by Nicholson and Halpern in bombardments of  $U^{238}$  with alpha particles.<sup>6</sup> Possible explanations for this are: (a) a wide spread in the momentum of the fissioning nucleus, (b) an admixture of other transfer reactions, and (c) internal motion of the nucleons in the  $O^{16}$ . Another interesting observation is that fission-fission coincidences are recorded with the detectors 180 deg apart even after corrections have been made for angular spread. The following factors contribute to this apparent "negative" momentum transfer: (a) internal motion of the nucleons in the  $O^{16}$ , (b) evaporation of neutrons from the fission fragments, (c) admixture of reactions with small momentum transfer, such as  $n$  and  $p$  nucleon transfer and Coulomb excitation, and (d) scattering in the target

<sup>15</sup> T. Sikkeland, S. G. Thompson, and A. Ghiorso, *Phys. Rev.* **112**, 543 (1958).

<sup>16</sup> A. Ghiorso and T. Sikkeland, in *Proceedings of the Second Conference on the Peaceful Uses of Atomic Energy, Geneva, 1958* (United Nations, New York, 1958), Vol. 14, p. 158.

<sup>17</sup> A. Ghiorso, T. Sikkeland, A. E. Larsh, and R. M. Latimer, Lawrence Radiation Laboratory (unpublished work).

<sup>18</sup> H. C. Britt and A. R. Quinton, *Phys. Rev.* **124**, 877 (1961).

and backing. (Comparison of 750- $\mu\text{g}/\text{cm}^2$  and 250- $\mu\text{g}/\text{cm}^2$  targets indicates that this effect is negligible.)

The presence of transfer reactions was confirmed in the following way. The dominant  $\alpha$ -particle transfer reaction can be written  $\text{U}^{238}(\text{O}^{16}, \text{C}^{12})\text{Pu}^{242*}$ , whereas the CN reaction is  $\text{U}^{238}(\text{O}^{16})\text{Fm}^{254*}$ . These two nuclei decay predominantly by fission. Since neutron evaporation dominates over charged-particle evaporation,<sup>18,19</sup> we should expect the fragments that enter the detectors when the system is at the CN peak to be coming from fissioning Fm isotopes. Similarly, at the NCN peak, we should see fission from Pu isotopes. One detector was first fixed at 64.5 deg with geometry corresponding to the peak for the CN reaction, and the energy spectrum of the coincident fragments was observed in the other detector—at 90 deg. The most probable energy was found to be 93 Mev (c.m.). The first detector was then set at 81.5 deg and the most probable kinetic c.m. energy of the fragments entering the detector at 90 deg was found to be 85.5 Mev. These are reasonable values for the elements in question.

It is interesting to note that the same procedure can be used to measure the angular distribution of the fragments from the CN reactions. By adjusting the relative positions of the two detectors, one can practically exclude fragments originating in undesired reactions from entering the detectors.

<sup>19</sup> E. Hubbard, R. Main, and R. Pyle, Phys. Rev. **118**, 507 (1960).

## CONCLUSION

The method used in this investigation is useful for measuring directly and with a high degree of accuracy the  $x_{mp}^2$  values for reactions leading to fission. Estimated  $x_{\text{CN}}^2$  values agree very well with the  $x_{mp}^2$  measured for several combinations of targets and heavy ions. The dominant reaction appears to be one in which the heavy ion deposits its full momentum. Evidence is also presented for reactions with incomplete momentum transfer. We have estimated the relative amounts of these NCN reactions contributing to fission. For  $\text{Ne}^{20} + \text{Au}^{197}$  and  $\text{Ne}^{20} + \text{Bi}^{209}$  large fractions of the momentum, corresponding to eight or more nucleons, are transferred. With a  $\text{U}^{238}$  target the dominant NCN reaction is an  $\alpha$ -particle transfer reaction. The momentum of the fissioning nucleus in this case has a wider spread than the momentum of the nucleus in a CN reaction and its most probable momentum is higher than that of an  $\alpha$ -particle with the same velocity as the projectile.

## ACKNOWLEDGMENTS

The excellent design of the chamber was done by Charles A. Corum. We are very thankful for the help of Almon E. Larsh, Leonard E. Gibson, and William W. Goldsworthy with the electronics. Robert Latimer furnished us with the indispensable silicon detectors. We are grateful to the Hilac crew for the good beams of ions through many hours of running time. Daniel G. O'Connell was most helpful in preparing some of the targets used in the experiments.



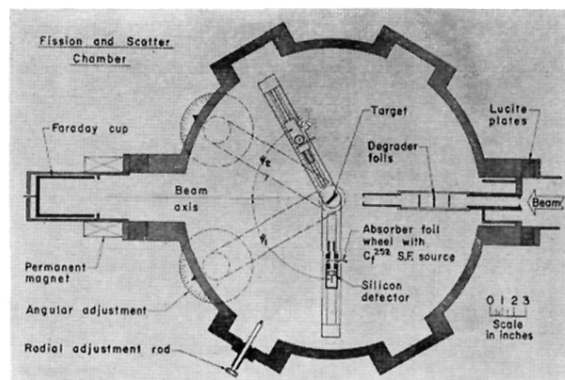


FIG. 2. Schematic diagram of the fission and scatter chamber.